JOURNAL OF MATERIALS SCIENCE **34** (1999) 951–955

Crystallization behavior of amorphous solid solutions and phase separation in the Cr_2O_3-Fe_2O_3 system

Y. MURAKAMI, A. SAWATA, Y. TSURU
Advanced Technology Research Center, Mitsubishi Heavy Industries, Ltd., Sachiura 1-8-1, Kanazawa-ku, Yokohama 236-8515, Japan
E-mail: murakami@atrc.mhi.co.jp

Fine particles of the amorphous Cr_2O_3-Fe_2O_3 solid solutions were prepared by dehydration of coprecipitated hydroxides and their crystallization behavior was studied by differential thermal analysis and X-ray diffraction. The peak temperature for crystallization attained a maximum at a composition near Fe_2O_3 content of about 60 mol % and the activation energy for crystallization attained a minimum at a composition near Fe_2O_3 content of about 50 mol % in this quasibinary system. Phase separation occurred in a range of Fe_2O_3 content from about 35 to 80 mol % in the corundum-type solid solutions heat treated at 600 °C for 2 h. Crystallization behavior was discussed briefly related with phase separation and diffusion in fine particles.

1. Introduction

Oxide solid solutions of the Cr_2O_3-Fe_2O_3 system are promising for application in engineering materials such as passive films [1], catalysts [2, 3], magnetic recording materials, refractory materials and abraisives [3–5]. In the Cr_2O_3-Fe_2O_3 solid solutions with corundum structure, composition dependence of internal magnetic field, Fourier transform infrared (FT-IR) spectra and lattice parameters has been reported by many investigators [3–6].

As an interesting problem, phase separation has been reported to occur in the Cr_2O_3-Fe_2O_3 solid solutions prepared by solid state reaction [4]. On the other hand, continuous solid solutions have been reported to occur in the powder specimens prepared by other method such as sol-gel and mechanical treatment of coprecipitated hydroxides [3, 5, 6]; these solid solutions might be metastable because of the possibility of phase separation. These discrepancies concerning the region of continuous solid solutions in this system are considered to be affected by the preparation method of specimens and the characterization technique.

Curry-Hyde and Baiker have shown that amorphous Cr_2O_3 has high activity for low temperature selective catalytic reduction of nitric oxide [2]. Thereby, investigation of the property of amorphous oxide solid solutions seems to be important for a practical application. Tsokov and coworkers [5] have shown that the peak temperature for crystallization, T_0, in Fe_2O_3 powder tends to rise by the addition of Cr_2O_3. However, details of the composition dependence of T_0 in this quasibinary system are not clear.

Then, in this work, crystallization behavior in amorphous solid solutions and phase separation in crystalline solid solutions in the Cr_2O_3-Fe_2O_3 system have been studied.

2. Experimental

The raw materials used were $Cr(NO_3)_3 9H_2O$ and $Fe(NO_3)_3 9H_2O$ with 99.9% purity. The mixed hydroxides with definite composition were prepared by the chemical coprecipitation method adding 2 kmol/m^3 NH_4OH to the aqueous solution containing 0.5 kmol/m^3 $Me(NO_3)_3$, where Me represents the mixture of Cr^{3+} and Fe^{3+} depending on composition. The precipitates of mixed hydroxides were washed carefully and dried at 120 °C for 20 h. These dried powders were heat treated at 300 °C for 2 h to prepare the fine powders of amorphous solid solutions, and then heat treated at 600 °C for 2 h to prepare those of crystalline solid solutions.

The temperature for dehydration and the peak temperature for crystallization were determined by differential thermal analysis (DTA): the dried powders of mixed hydroxides were heated at a heating rate of 5 °C/min using a Rigaku-TAS200 differential thermal analyzer. Crystal structure was determined by X-ray diffraction (XRD) using a Rigaku-RAD diffractometer with monochromatized CuK_α radiation. Crystallization behavior was observed by analyzing XRD patterns of specimens heat treated at various temperatures using a step scanning technique. FT-IR spectra were observed at room temperature using a JEOL FT-IR spectrophotometer. Morphology of oxide powders was observed by transmission electron microscopy (TEM) using a JEOL 2000FX instrument operated at 200 kV.

The heating rate of specimen for DTA was varied from 2 to 11 °C/min and the activation energy for

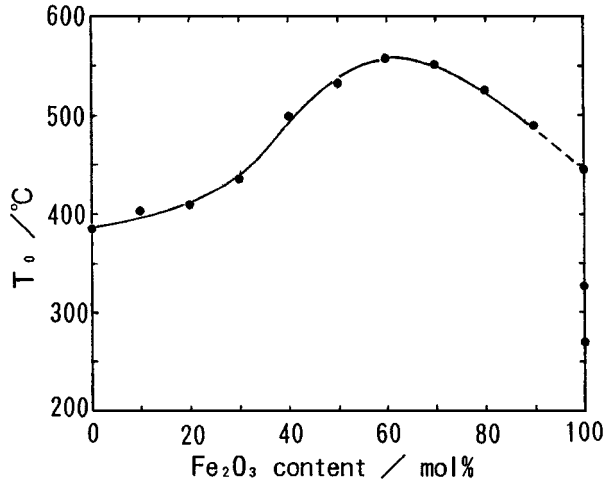

Figure 1 Peak temperature for crystallization, T_0, in the amorphous Cr_2O_3-Fe_2O_3 solid solutions as a function of Fe_2O_3 content.

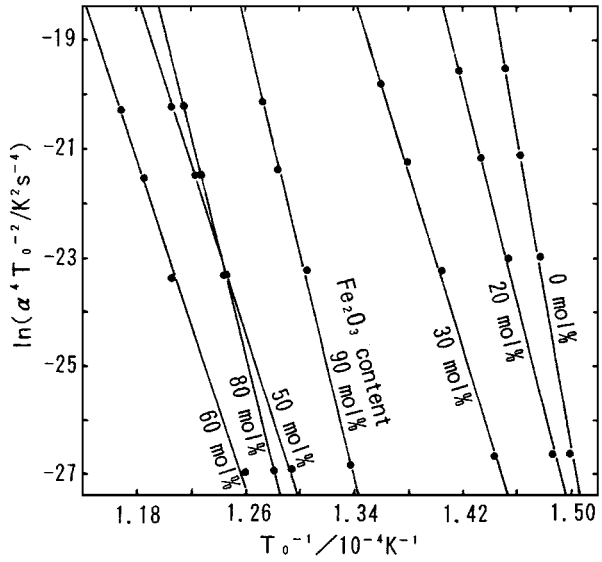

Figure 2 $\ln(\alpha^4/T_0^2)$ vs. T_0^{-1} plot representing a relation between peak temperature for crystallization, T_0, and heating rate, α, in DTA in the amorphous Cr_2O_3-Fe_2O_3 solid solutions.

crystallization were determined by analyzing the heating rate dependence of T_0 in the powder specimen of amorphous solid solution [7, 8].

3. Results and discussion

3.1. Thermal analysis

During heating the specimen of coprecipitated hydroxides up to 700 °C by DTA, an endothermal peak due to dehydration and an exothermal peak due to crystallization were observed. These are similar to those reported by Tsokov *et al.* [5] and details of DTA curves are omitted for simplicity. In hydroxides of the quasibinary $Cr(OH)_3$-$Fe(OH)_3$ system, the finishing temperature for dehydration during heating tended to rise with increasing $Fe(OH)_3$ content, e.g. it was 195 °C in $Cr(OH)_3$ and 215 °C in $Cr_{0.1}Fe_{0.9}(OH)_3$ composition.

Fig. 1 represents the peak temperature for crystallization, T_0, in the amorphous Cr_2O_3-Fe_2O_3 solid solutions as a function of Fe_2O_3 content. T_0 vs. composition curve has a maximum at a composition near $(Cr_2O_3)_{40}$ $(Fe_2O_3)_{60}$. Only in powder specimen with Fe_2O_3 composition, three exothermal peaks were observed as shown in Fig. 1; this phenomenon might be affected by the formation of other phases such as α-FeOOH and γ-Fe_2O_3 below 445 °C [4, 9]. Thus, formation process of the corundum-type phase in the end member of Fe_2O_3 is considered to be different from that in the Cr_2O_3-Fe_2O_3 solid solutions, and then, detailed investigation was not carried out in Fe_2O_3 composition in this study. Broken line in Fig. 1 represents the extrapolation of T_0 to the end member of Fe_2O_3.

Usually, T_0 rises with increasing heating rate, α, in DTA [7, 8]. Matusita and Sakka [7] have proposed that the relation between T_0 and α is given by the following equation:

$$\ln(\alpha^m/T_0^2) = \text{const} - n\Delta E_{cr}/kT \qquad (1)$$

Here, ΔE_{cr} is the activation energy for crystallization, m and n are the constants depending on nucleation mechanism. They have proposed $m = 4$ and $n = 3$ in the case of three dimensional volumetric nucleation [7].

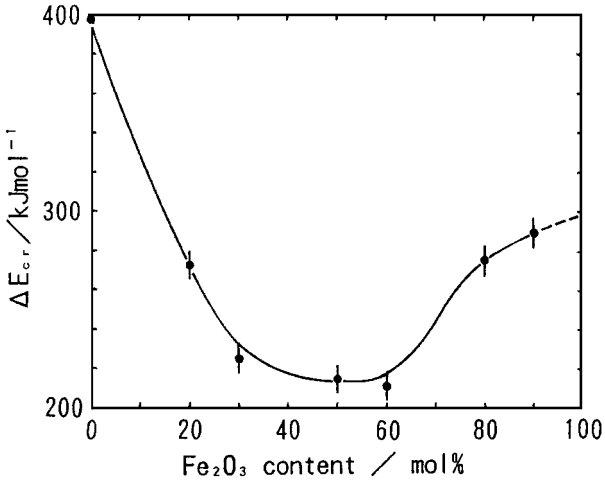

Figure 3 Activation energy for crystallization, ΔE_{cr}, in the amorphous Cr_2O_3-Fe_2O_3 solid solutions as a function of Fe_2O_3 content.

Fig. 2 represents $\ln(\alpha^4/T_0^2)$ vs. T^{-1} relations in the amorphous Cr_2O_3-Fe_2O_3 solid solutions obtained by DTA. By measuring the slope of this line, ΔE_{cr}-value can be determined.

The activation energy for crystallization, ΔE_{cr}, in the Cr_2O_3-Fe_2O_3 system is shown in Fig. 3 as a function of Fe_2O_3 content. ΔE_{cr} vs. composition curve has a minimum at a composition near $(Cr_2O_3)_{50}$ $(Fe_2O_3)_{50}$. Broken line shows the extrapolation of ΔE_{cr}-value to the end member of Fe_2O_3.

3.2. Sample characterization

FT-IR spectra of the amorphous Cr_2O_3-Fe_2O_3 solid solutions heat treated at 300 °C for 2 h are shown in Fig. 4. In the amorphous solid solutions, the absorption bands, which are located at 544 and 948 cm^{-1} in Cr_2O_3 composition, shift towards lower wave numbers with increasing Fe_2O_3 content and they are located at 457 and 935 cm^{-1}, respectively, in $(Cr_2O_3)_{10}$ $(Fe_2O_3)_{90}$ composition. This result suggests that the solid solutions

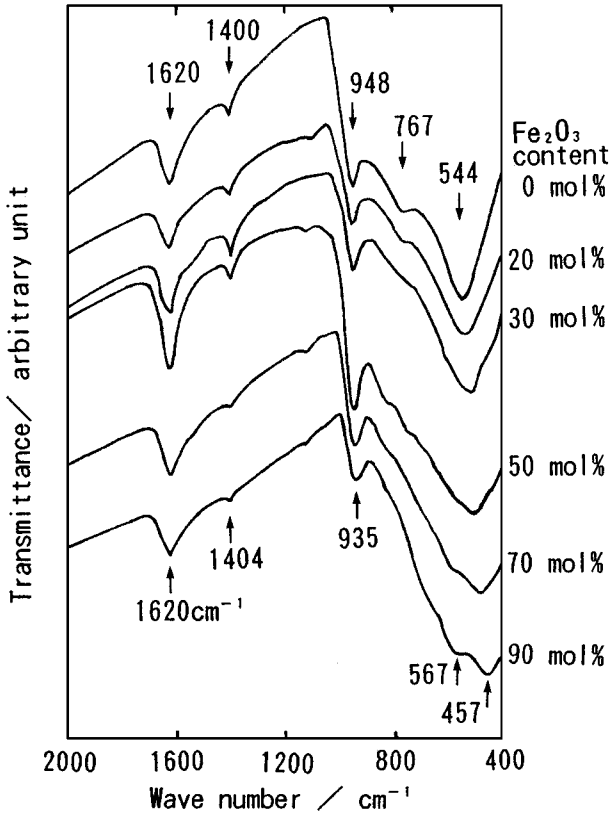

Figure 4 FT-IR spectra of amorphous Cr_2O_3-Fe_2O_3 solid solutions heat treated at 300 °C for 2 h.

are obtained in the Cr_2O_3-Fe_2O_3 system. Extra shoulders were observed at a wave number near 767 cm^{-1} in Cr_2O_3-rich solution and at a wave number near 567 cm^{-1} in Fe_2O_3-rich solution in Fig. 4. FT-IR absorption bands of amorphous solid solutions shown in Fig. 4 seem to be broader than those of crystalline solid solutions reported by several investigators [3–5].

3.3. Crystallization and phase separation

In specimens heat treated at 600 °C for 2 h, the crystalline Cr_2O_3-Fe_2O_3 solid solutions with corundum structure have been obtained. XRD peaks with (214) and (300) indices, which are located at diffraction angle (2θ) near about 62° and 64°, respectively, separate into two peaks, suggesting the occurrence of phase separation. These XRD patterns are similar to those reported by Music and coworkers [4].

Fig. 5 shows the composition dependencee of interplanar spacings, d_{214} and d_{300}, of the corundum structure in Cr_2O_3-Fe_2O_3 solid solutions heat treated at 600 °C for 2 h, which has been determined by measuring the diffraction angles of (214) and (300) XRD peaks using a step scanning technique. Both d_{214} and d_{300} increase with increasing Fe_2O_3 content in a range of Fe_2O_3 content from 0 to about 35 mol % and similarly from about 80 to 100 mol % as shown by solid lines in Fig. 5, where the continuous solid solutions are obtained. By analyzing the composition dependence of d_{214} and d_{300} in Fig. 5, it is considered that the phase separation into Cr_2O_3-rich and Fe_2O_3-rich solid solutions occurs in a range of Fe_2O_3 content from about 35 to 80 mol %. The broken lines in Fig. 5 represent the two phase region.

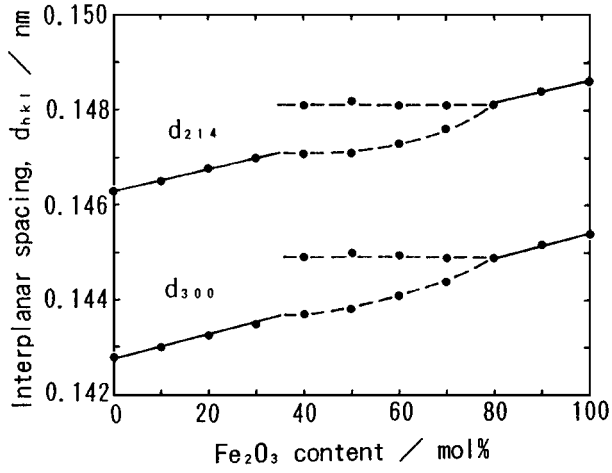

Figure 5 Interplanar spacings, d_{214} and d_{300}, of the corundum structure in Cr_2O_3-Fe_2O_3 solid solutions heat treated at 600 °C for 2 h as a function of Fe_2O_3 content.

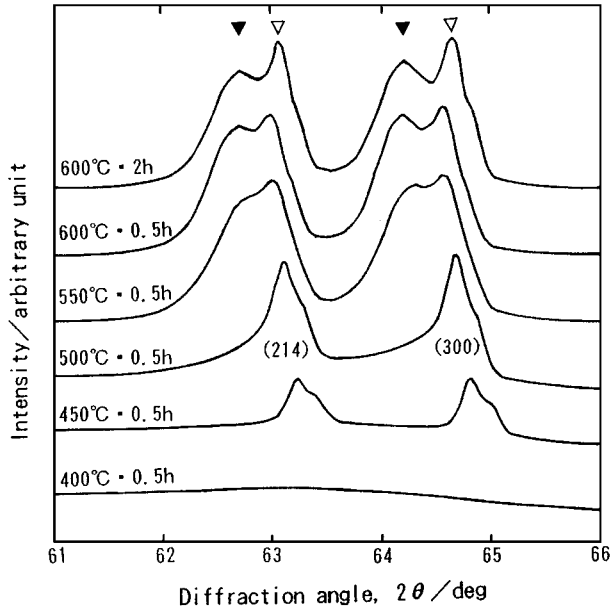

Figure 6 XRD patterns of $(Cr_2O_3)_{40}$ $(Fe_2O_3)_{60}$ powder specimens heat treated at various temperatures. ▽ and ▼ represent XRD peak for Cr_2O_3-rich solid solution and that for Fe_2O_3-rich solid solution, respectively.

Crystallization behavior of the amorphous $(Cr_2O_3)_{40}$ $(Fe_2O_3)_{60}$ powder specimen was observed by XRD using a step scanning technique. XRD patterns of the specimens heat treated at various temperatures are revealed in Fig. 6. A specimen heat treated at 400 °C for 0.5 h is considered to be amorphous as shown in Fig. 6. In a specimen heat treated at 450 °C for 0.5 h, XRD peaks appear at diffraction angles near about 63.1° and 64.7°, suggesting that the nucleation and growth of Cr_2O_3-rich crystals occur preferentially at an early stage of crystallization. In a specimen heat treated at 550 °C for 0.5 h, additional XRD peaks appear at diffraction angles near about 62.6 °C and 64.2 °C, suggesting that the nucleation and growth of Fe_2O_3-rich crystals occur together with that of Cr_2O_3-rich crystals. From these results, crystallization process in this specimen is considered as follows: (i) during heating, onset of crystallization of Cr_2O_3-rich crystals occurs at first, and accordingly, the composition of matrix is

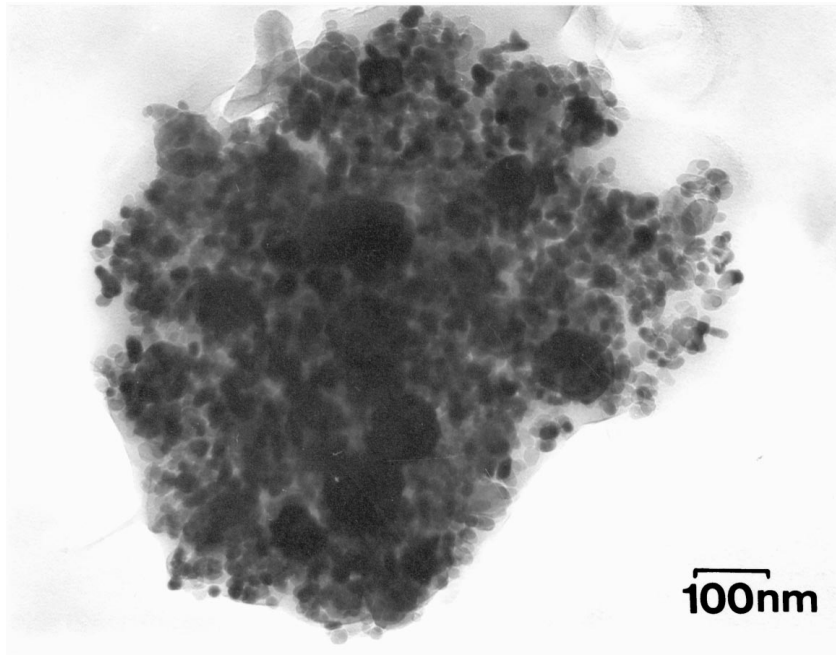

Figure 7 Transmission electron micrograph of $(Cr_2O_3)_{40}$ $(Fe_2O_3)_{60}$ powder specimen heat treated at 600 °C for 2 h.

suggested to shift towards higher Fe_2O_3 concentration, and (ii) during further heating, onset of crystallization of Fe_2O_3-rich crystals occurs in the matrix with high Fe_2O_3 content and both Fe_2O_3-rich and Cr_2O_3-rich crystals grow, which results in the phase separation. As an interesting problem in Fig. 6, (214) and (003) XRD peaks of Cr_2O_3-rich crystals shifts towards higher diffraction angles with decreasing temperature. This result suggests that the solubility of Fe_2O_3 into Cr_2O_3 tends to decrease with decreasing temperature.

Fig. 7 reveals a TEM micrograph of $(Cr_2O_3)_{40}$ $(Fe_2O_3)_{60}$ powder specimen heat treated at 600 °C for 2 h. In this specimen, size of mother particles was distributed from about 10 to 1500 nm. In Fig. 7, grobular daughter crystallites with about 10–40 nm in size were grown in a mother particle of about 700 nm in size. This result suggests that the crystallization occurs by the nucleation and growth mechanism in this specimen. This is similar with the crystallization behavior of amorphous $Al_{1.8}Fe_{0.2}O_3$ particles [9].

3.4. Crystallization behavior

In the present amorphous solid solutions, T_0 attains a maximum and ΔE_{cr} attains a minimum at a composition near equimolar composition. This property is different from that of oxide glasses. For example, in the Yb-Si-Al-O glasses of the quasibinary $Yb_2Si_2O_7$-$Al_6Si_2O_{13}$ system, both T_0 and ΔE_{cr} have been reported to attain a maximum at an eutectic composition ($Al_6Si_2O_{13}$ content: 54.5 mol %) [8]. Because the free energy of glassy phase is suggested to decrease at a composition near the eutectic composition by the contribution of mixing entropy, the glassy phase might become stable at a composition near the eutectic composition [8].

Regarding the diffusion in oxides, the activation energies for diffusion of Cr^{3+} and O^{2-} ions have been reported to be 256 kJ/mol [10] and 423 kJ/mol [11], respectively, in Cr_2O_3 crystal. As shown in Fig. 3, in amorphous Cr_2O_3 powder specimen, ΔE_{cr} is 398 kJ/mol, which is in the same order with that for diffusion of O^{2-} ions in Cr_2O_3 crystal [11]. This result suggests that the diffusion of O^{2-} ions has an important role on the crystallization in Cr_2O_3 composition. However, in Fe_2O_3-rich composition, ΔE_{cr} is fairly smaller than those (419 kJ/mol [12] and 611 kJ/mol [13], respectively) for diffusion of Fe^{3+} and O^{2-} ions in α-Fe_2O_3 crystal. This result suggests that the diffusion in amorphous fine particles occurs easily and that the large amount of free volume occurs in amorphous fine particles. Moreover, in this quasibinary system, ΔE_{cr} attains a minimum at the equimolar $(Cr_2O_3)_{50}$ $(Fe_2O_3)_{50}$ composition. Because O^{2-} ions and two kinds of cations with different ionic radius are mixed in this system, the amount of free volume might increase as the composition approaches to the equimolar composition in amorphous fine particles; this may be a reason for the minimum of ΔE_{cr} in Fig. 3.

In specimens with smaller ΔE_{cr}-value, it is considered that crystallization may occur at lower temperature. On the contrary, in the present quasibinary system, T_0 attains a maximum at a composition near $(Cr_2O_3)_{40}$ $(Fe_2O_3)_{60}$ as shown in Fig. 1. The mixing entropy is considered to increase at an equimolar composition in amorphous phase, which may affect the stabilization of amorphous phase. However, reason for the maximum of T_0 is still unclear in this system.

4. Conclusion

In the amorphous Cr_2O_3-Fe_2O_3 solid solutions, the peak temperature for crystallization attains a maximum at a composition near $(Cr_2O_3)_{40}$ $(Fe_2O_3)_{60}$. The activation energy for crystallization attains a minimum at a composition near $(Cr_2O_3)_{50}$ $(Fe_2O_3)_{50}$. In the

corundum-type Cr_2O_3-Fe_2O_3 solid solutions heat treated at 600 °C for 2 h, phase separation occurs in a range of Fe_2O_3 content from about 35 to 80 mol %. In this range of composition, crystallization in amorphous solid solutions occurs followed by phase separation.

References

1. P. SCHMUKI, S. VIRTANEN, H. S. ISAACS, M. P. RYAN, A. J. DAVENPORT, H. BÖHNI and T. STENBERG, *J. Electrochem. Soc.* **145** (1998) 791.
2. E. CURRY-HYDE and A. BAIKER, *Ind. Eng. Chem. Res.* **29** (1990) 1985.
3. S. MUSIC, S. POPOVIC and M. RISTIC, *J. Mater. Sci.* **28** (1993) 632.
4. S. MUSIC, M. LENGLET, S. POPOVIC, B. HANNOYER, I. C. NAGY, M. RISTIC, D. BALZAR and F. GASHI, *ibid.* **31** (1996) 4067.
5. P. TSOKOV, V. BLASKOV, D. KLISSURSKI and I. TSOLOVSKI, *ibid.* **28** (1993) 184.
6. A. K. BHATTACHARTA, A. HARTRIDGE, K. K. MALLICK, C. K. MAJUMUDAR, D. DAS and S. N. CHINTALAPUDI, *ibid.* **32** (1997) 557.
7. K. MATUSITA and S. SAKKA, *J. Non-Cryst. Solids* **38** (1980) 741.
8. Y. MURAKAMI and H. YAMAMOTO, *J. Ceram. Soc. Jpn.* **101** (1993) 1101.
9. A. D. POLLI, F. F. LANGE and G. G. LEVI, *J. Amer. Ceram. Soc.* **79** (1996) 1745.
10. W. C. HAGEL and A. U. SEYBOLT, *J. Electrochem. Soc.* **108** (1961) 70.
11. W. C. HAGEL, *J. Amer. Ceram. Soc.* **48** (1965) 70.
12. V. I. IZVEKOV, N. S. GORBUNOV and A. A. BABAD-ZAKHRYAPIN, *Fiz. Metal. Metalloved.* **14** (1962) 195.
13. W. D. KINGERY, D. C. HILL and R. P. NELSON, *J. Amer. Ceram. Soc.* **49** (1966) 244.

Received 31 July
and accepted 14 October 1998